Manish Singh <sup>®</sup> ; Lakshmi Narayanan Ramasubramanian <sup>®</sup> ; Raj N. Singh ■ <sup>®</sup>



Journal of Vacuum Science & Technology B 41, 042208 (2023) https://doi.org/10.1116/6.0002749





CrossMark



Cite as: J. Vac. Sci. Technol. B **41**, 042208 (2023); doi: 10.1116/6.0002749 Submitted: 10 April 2023 · Accepted: 5 June 2023 ·







Published Online: 30 June 2023

Manish Singh, Dakshmi Narayanan Ramasubramanian, Dand Raj N. Singh Raj N.

## **AFFILIATIONS**

<sup>1</sup>School of Materials Science and Engineering, Oklahoma State University, 700 N. Greenwood Avenue, Tulsa, Oklahoma 74106

a) Author to whom correspondence should be addressed: rajns@okstate.edu

#### **ABSTRACT**

There is a growing need for digital and power electronics to deliver higher power for applications in batteries for electric vehicles, energy sources from wind and solar, data centers, and microwave devices. The higher power also generates more heat, which requires better thermal management. Diamond thin films and substrates are attractive for thermal management applications in power electronics because of their high thermal conductivity. However, deposition of diamond by microwave plasma enhanced chemical vapor deposition (MPECVD) requires high temperatures, which can degrade metallization used in power electronic devices. In this research, titanium (Ti)–aluminum (Al) thin films were deposited by DC magnetron sputtering on p-type Si (100) substrates using a physical mask for creating dot patterns for measuring the properties of the contact metallization. The influence of processing conditions and postdeposition annealing in argon (Ar) and hydrogen (H<sub>2</sub>) at 380 °C for 1 h on the properties of the contact metallization is studied by measuring the I-V characteristics and Hall effect. The results indicated a nonlinear response for the as-deposited films and linear ohmic contact resistance after postannealing treatments. In addition, the results on contact resistance, resistivity, carrier concentration, and Hall mobility of wafers extracted from Ti–Al metal contact to Si (100) are presented and discussed.

Published under an exclusive license by the AVS. https://doi.org/10.1116/6.0002749

### I. INTRODUCTION

The development of thin film technology has been an area of high scientific activities and industrial interest for enhancing optical, electrical, magnetic, chemical, and mechanical properties of bulk materials.<sup>1-4</sup> Innovative thin film processing methods are also developed to meet the constantly increasing demands of industries and other sectors. 1,3 These thin film materials/technologies have been widely used in different areas such as lithography, microelectromechanical systems (MEMS), semiconductor devices, wireless communications, integrated circuits, rectifiers, transistors, solar cells, light emitting diodes, photoconductors, and crystal display systems.<sup>5,6</sup> For example, aluminum (Al) thin film, which shows superior properties of low resistivity, low cost, high availability, and high adhesion to different substrates, has gained attention in areas such as integrated circuits, semiconductor devices, liquid crystal display systems, and transistors.<sup>3,7,8</sup> Also, aluminum films are extensively used in optical devices, such as front or reflective surfaces of MEMS mirrors and solar cells because of good reflectivity.<sup>3,7</sup>

For electronic applications, Al thin films are mostly deposited on silicon (Si) and silicon oxide (SiO<sub>2</sub>) substrates.

Thin aluminum film deposition is accomplished through physical and chemical methods by varying deposition conditions, parameters, and substrates.<sup>2</sup> The physical methods are better than the chemical methods because of good adhesion, lower substrate temperatures, and environmentally friendly processing. Further, physical deposition techniques can also be used to deposit thinner, metastable films, and control stress states. Physical methodologies of vacuum evaporation, magnetron sputtering, <sup>9–11</sup> electron beam evaporation, <sup>12</sup> and thermal arc spray<sup>13</sup> are used to deposit Al thin films on different substrates. Magnetron sputtering is regarded as the most advantageous of these physical methods because it can be used to deposit thin films over a large area with a relatively high deposition rate. Furthermore, better optical properties have been obtained for solar selective coatings using sputtering technology.<sup>4,14</sup>

Si and wide bandgap semiconductors have been extensively used to fabricate high-power and high-frequency electronics devices,

such as field-effect transistor, high electron mobility transistors, heterojunction bipolar transistors, and laser diodes. The trend toward smaller device size, higher output power, higher frequency, and high-performance of Si and wide bandgap semiconductor-based power electronic devices are increasing and remain irreversible. However, these Si based devices generate large amounts of heat and often exhibit nonuniform heat dissipation, causing them to reach excessive temperatures that can degrade their performance, reliability, and lifetime. To improve heat dissipation and to solve the degradation of device performance and reliability, it is of utmost importance to reduce thermal resistance, and materials with high thermal conductivity and low thermal expansion are needed for a better thermal management. 15-21

Thin film diamond is considered an attractive material for the thermal management of semiconductor electronics owing to its outstanding optical, electrical, mechanical, and thermal prop-Diamond has high thermal conductivity (2000 W/m K), a large band gap (5.47 eV), and a large breakdown electric field  $(2 \times 10^{-7} \text{ V cm}^{-1})$ . Also, diamond is an electrical insulator but at the same time, it is an excellent thermal conductor, which is being explored to remove heat generated in electronic devices. Among the diamond deposition processes, the hot filament chemical vapor deposition and the MPECVD methods have proven to be the most widely used diamond deposition processes for producing high-quality diamond films. However, high temperature diamond synthesis comes with limitations. For electronic devices, low-temperature diamond synthesis (<400 °C) is desirable to avoid damage to metallization. However, it is still unclear from the literature whether the metallization of the device will be degraded by the deposition of a diamond thin film on Si. Our team has conducted research on the processing of diamond thin films for thermal management of GaN-based power electronics with Ni/Au metallization at temperatures below 400 °C.10

Aluminum can form ohmic contact with p-type Si (100), but when heated to 400 °C silicon can react with Al and can form pits and affect contact metallization. In the case of severe Si-Al reaction, failures at the junction and contact metallization may occur. In order to solve this problem, a diffusion barrier of Ti is placed between Si and Al. Titanium thin films have long been used as a successful diffusion barrier as well as adhesion promotor in semiconductor technology due to their high thermal and chemical stability as well as low electrical resistivity. Because of these characteristics, Ti provides stability to the repeated thermal cycles present in the multistep manufacturing processes of integrated circuit devices.

The objectives of this paper are processing and measuring the electrical properties of Ti-Al metal contact on p-Si (100). The processing was done using DC magnetron sputtering technique, and Hall measurements in a Van Der Pauw configuration<sup>24,25</sup> were used to determine the electrical properties of Si substrate at room temperature. The results were analyzed for determining the nature of the metal-Si contact resistance from I-V data, and resistivity, career concentration, Hall mobility, and Hall coefficient of the Si substrate. In addition, Ti-Al metal contact on Si was subjected to postannealing treatments in Ar and H2 atmospheres at 380 °C for 1 h, and the I-V characteristic and electronic properties were determined after postannealing in Ar and H<sub>2</sub> environments.

### II. EXPERIMENT

## A. Deposition of Ti-Al contacts on Si (100) wafer using a 2 × 2 in.2 metal mask

Titanium (Ti) and aluminum (Al) films were sequentially sputtered on p-type silicon (100) wafer substrate using a DC magnetron sputtering system (Model # ATC ORION 8 Sputtering System from AJA INTERNATIONAL, Inc.), which is a Five-gun system. DCXS-750-4 Multiple Sputter Source DC Power Supply was used for sputtering. The sputter chamber was evacuated to a base pressure lower than  $10^{-7}$  Torr using a turbomolecular pump and a rotary pump. Ti and Al targets (99.9% pure) with a diameter of 2 in. and a thickness of 0.25 in., respectively, were employed as the sputter targets. Argon (Ar) gas (of 99.9% purity) was used as the sputtering gas with a constant flow rate of 20 sccm. The chamber pressure was measured by ion-gauge and the argon gas pressure was controlled by the throttle valve. Before deposition, Si (100) substrate was ultrasonically cleaned with acetone for 5 min and rinsed with water. Then, it was ultrasonically etched with 5% HF for 5 min to remove the native oxide layer on the substrate surface followed by rinsing with water and isopropyl alcohol. To ensure the purity of the films, presputtering of Ti and Al targets was done. Pure argon (Ar) was used for presputtering to clean the surface of Al and Ti targets. The presputtering time for Ti and Al targets was 5 min each, and the presputtering power for Ti and Al targets was 50 and 350 W, respectively. Also, sputtering power was slowly increased by 10 W/10 s when the Ti and Al targets were presputtered. In addition, there was good circulation of cooling water to ensure continuous sputtering with high power without ointerruption. interruption.

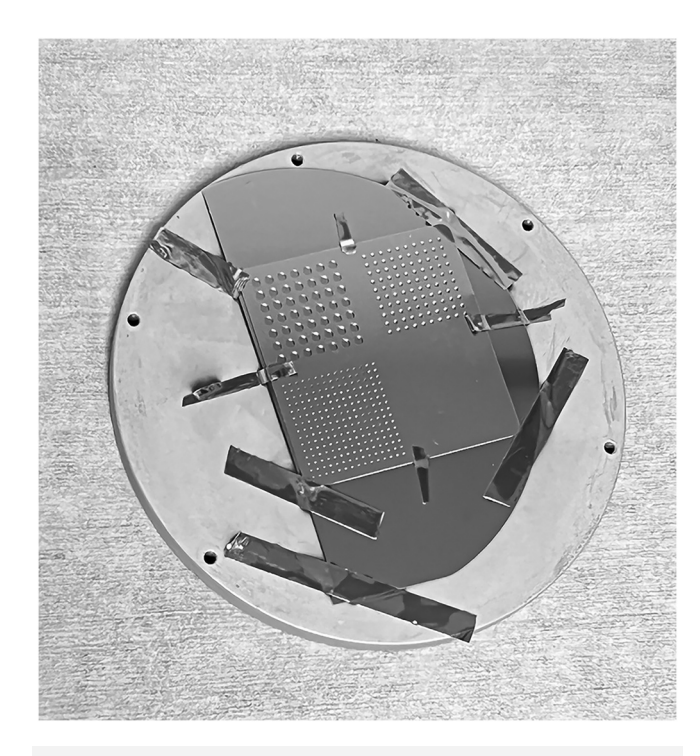
Substrates were rotated at 20 rpm during deposition for uniformity. Ti and Al films were sequentially deposited at the same deposition pressure (mTorr), different DC sputtering power (W), & and different deposition times as mentioned in Table I. Working distance between the target and substrate of 30 cm was used for all depositions. Also, a 2×2 in.2 mask was placed on top of the Si (100) wafer of 4 in. diameter as shown in Fig. 1 to create dot patterns of different sizes. We used very thin Ti layer ( $\sim$ 0.01  $\mu$ m) for ensuring good adhesion to Si substrate followed by the deposition of a relatively thicker Al film ( $\sim$ 1  $\mu$ m).

## B. Characterization of Ti-Al contact on Si (100) substrate using the Van der Pauw method

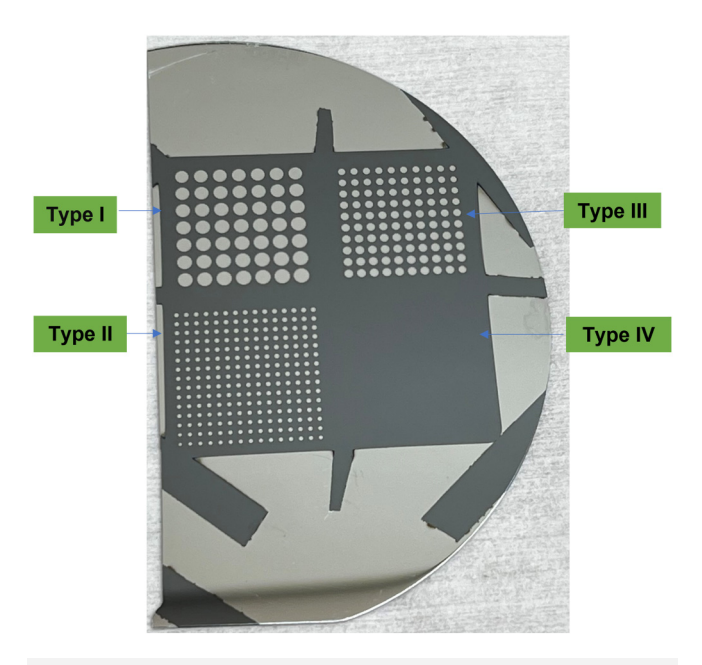
Before I-V and Hall measurements, smaller samples approximately  $\sim 1 \times 1$  in.<sup>2</sup> were obtained from a larger Ti-Al sample deposited on the Si (100) (Fig. 2) by cleaving into four parts and

TABLE I. Summary of DC magnetron sputtering conditions used for Ti and Al depositions sequentially.

Metal target	Pressure (mTorr)	Power (W)	Deposition time/thickness (min)/(μm)		
Titanium (Ti)	3	50	5/0.01		
Aluminum (Al)		350	30/1		



**FIG. 1.** Picture of the setup used to hold a  $2 \times 2$  in.<sup>2</sup> metal mask on Si (100) wafer on a sample holder.



**FIG. 2.** Photograph showing Ti–Al dots of different diameters deposited on Si (100) wafer. Ti–Al contact type I (2 mm), II (1 mm), III (0.5 mm), and IV (0.05 mm) are defined based on the diameter of the circular dot.



FIG. 3. (a) Continuous contact dot pattern and (b) corner contact dot pattern of Ti–Al type I on Si (100).

identified as Ti–Al contact type I, type II, type III, and type IV, depending on the circular dot size of the metal contact. Contact type I refers to the bigger contact size and contact type IV refers to the smallest contact type. For this paper, Ti–Al contact type I was used and explored. To measure I-V characteristics and Hall measurements, Ti–Al contact type I was broken into four square shaped samples  $\sim 1 \times 1 \text{ cm}^2$ , and each square sample was used for the measurements. Also, to measure Ti–Al contact type I, two different approaches were considered and used. First is the continuous contact and second is the corner contact as shown in Fig. 3. To measure I-V characteristics, an initial current of  $-10\,\mu\text{A}$  was applied. The final current was set to  $10\,\mu\text{A}$  and the step current used was  $1\,\mu\text{A}$ .

The electrical properties of the Ti–Al type I contact were studied using Hall measurements in the Van der Pauw configuration at room temperature from which resistivity, Hall coefficient, and Hall mobility were determined. p-Si (100) samples of thickness  $500\,\mu\mathrm{m}$  were used to carry out the Hall measurements. For variable magnetic field measurement, linear sweep field reversal was selected, and maximum and minimum fields were 250 and 50 mT, respectively. The field step used was 50 mT, and a constant current of  $10\,\mu\mathrm{A}$  was applied to the Ti–Al type I contact on Si (100).

### C. Annealing procedures

Annealing of the Ti–Al films deposited on Si (100) substrate was performed in a tube furnace. The Ti–Al films were annealed at 380 °C under an argon atmosphere. The Ti–Al film on Si substrate was placed in a quartz boat at the central zone of a horizontal three-zone tube furnace. The furnace was evacuated to  $10^{-5}$  Pa ( $\sim 7.5 \times 10^{-8}$  Torr) and purged by using N<sub>2</sub>. Then, the system was evacuated to  $10^{-5}$  Pa ( $\sim 7.5 \times 10^{-8}$  Torr) and purged with argon to reach atmospheric condition (760 Torr). The sample was heated to



380 °C and kept there for 1 h in a flowing argon atmosphere at a flow rate of 20 sccm. Then, the furnace was cooled down in the argon cover gas. Another set of the Ti–Al samples was annealed at 380 °C under pure hydrogen atmosphere following similar steps. The annealed samples were then characterized for electrical properties.

### **III. RESULTS AND DISCUSSION**

Ti–Al metal contacts on p-Si (100) were processed and the properties of these contacts were determined using I-V and Hall measurements as described earlier and the results are presented and discussed in Secs. III A and III B.

## A. Current-voltage (I-V) behaviors of Ti-Al type I contact on p-Si (100)

After DC magnetron sputtering, the Ti–Al contacts in the form of dot patterns are obtained on Si (100) wafer as shown in Fig. 2. As mentioned earlier, first a thin Ti layer (adhesion promoter) is deposited followed by a thicker Al layer. The I-V measurements used type I contact of 2 mm diameter on samples in the as-deposited state and after annealing in Ar or H<sub>2</sub> at 380 °C for 1 h.

The results for samples in the as-deposited state are given in data of Figs. 4 and 5, respectively, for the continuous and corner contacts measured between 1–2, 2–3, 3–4, and 4–1 probe locations. Figures 4(a)-4(d) show a nonlinear I-V response with a correlation

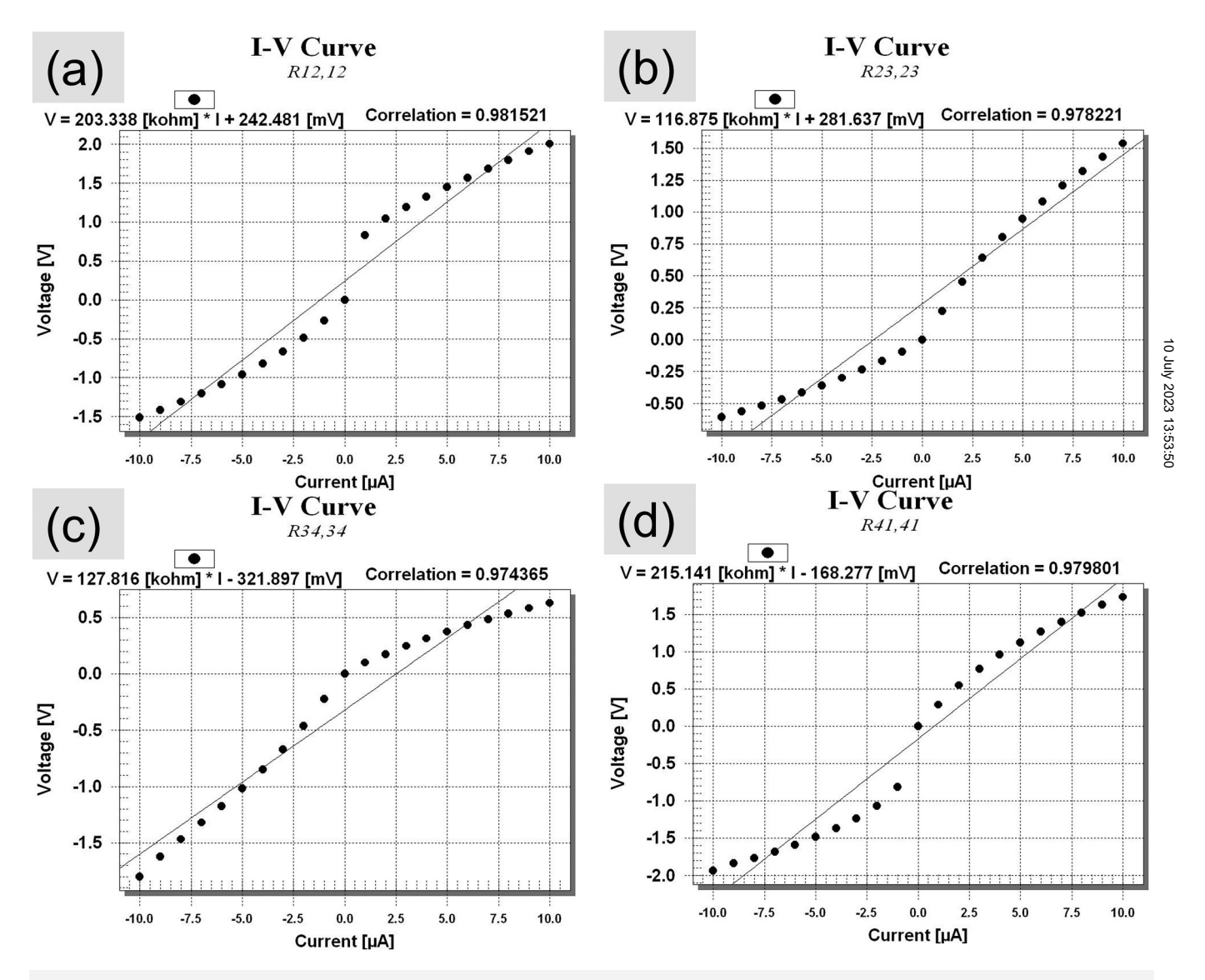


FIG. 4. I-V characteristics of Ti-Al continuous contact of type I on Si (100) in the as-deposited state between contacts (a) 1-2, (b) 2-3, (c) 4-1, and (d) 3-4.

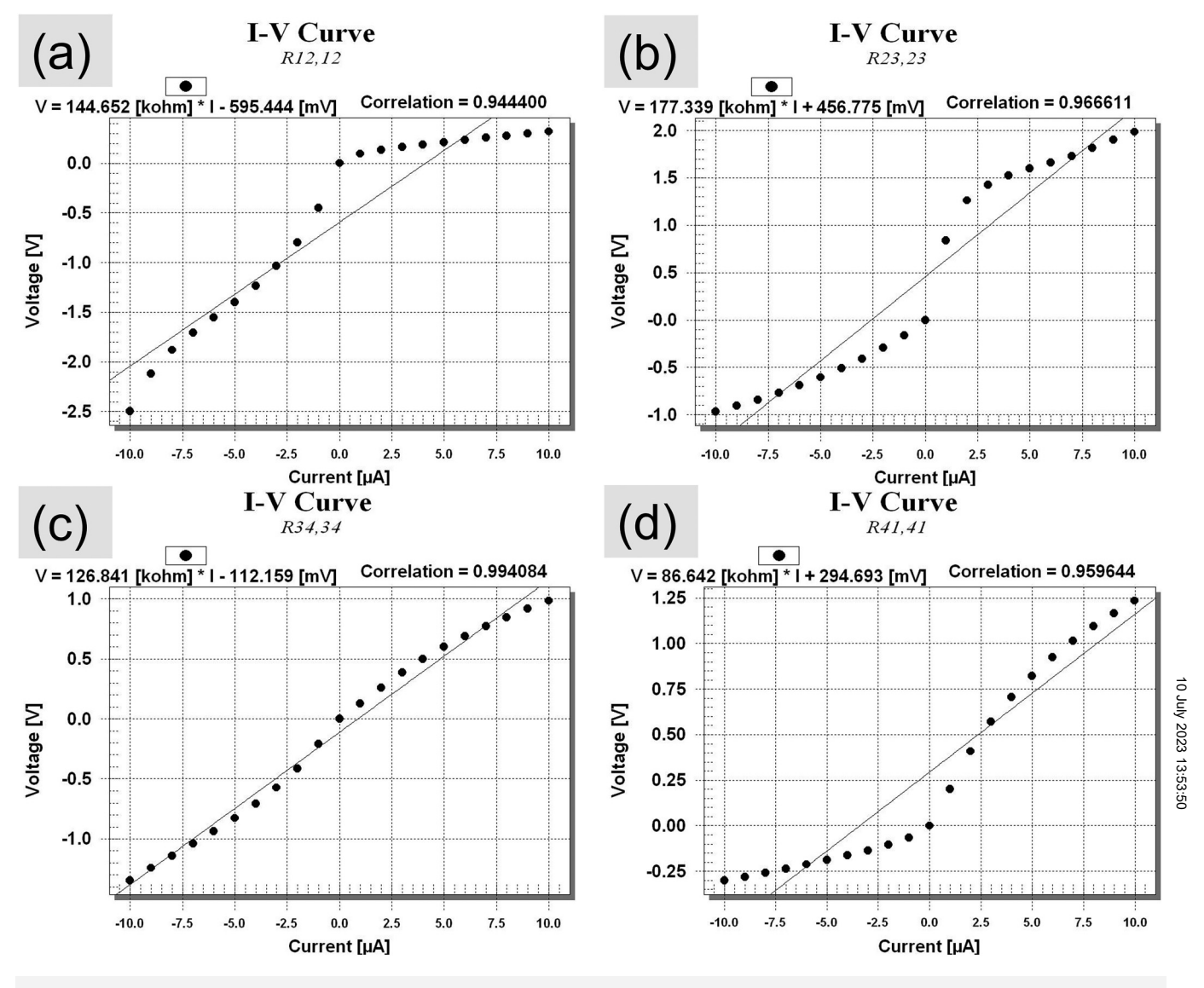


FIG. 5. I-V characteristics of Ti-Al corner contact of type I on Si (100) in the as-deposited state between contacts (a) 1-2, (b) 2-3, (c) 3-4, and (d) 4-1.

coefficient less than 1 indicating nonohmic contact measured on the continuous dot pattern. The results obtained for the corner contacts are given in Figs. 5(a)-5(d) and show a similar nonlinear response as the data of Fig. 4.

The deposition of Al film on Si substrates using DC magnetron sputtering is associated with some challenges such as interaction between the Al and Si substrate. When Al is sputtered on Si, the contact behaves in a rectifying fashion (nonohmic) and is associated with a high contact resistance. However, the Schottky–Mott rule predicts a low barrier height since there is a very small difference between the work function of Al and the electron affinity of Si ( $\approx 0.1-0.2 \, \text{eV}$ ). However, a high density of bandgap states or defects

at the Al/Si interface results in a high Schottky barrier height ( $\Phi B$ ) of  $\approx 0.65 \, \mathrm{eV}$  and blocks the flow of charges in/out of the Si wafer (Fermi-level pinning phenomenon). <sup>26–28</sup> We used the Ti layer for ensuring good adhesion to the Si substrate. However, the I-V characteristics of the Ti–Al corner/continuous type I contact to Si (100) show a nonlinear response in the as-deposited state.

To enhance interface adhesion and strength between Ti–Al and Si substrate, postannealing is done. The annealing process promotes adhesion and reduces any electrical damage caused during magnetron sputtering. Postannealing treatment (380 °C in Ar for 1 h) helps in limited solid-state diffusion of Al into the Si in the interface region. Al acts as an acceptor in p-Si and



TABLE II. Summary of electrical properties of p-Si (100) obtained from Hall measurement using continuous and corner contacts of Ti–Al metallization and effect of annealing in Ar and H<sub>2</sub> atmospheres at 380 °C for 1 h.

Ti-Al contact processing condition	Resistivity (Ohm cm)		Carrier concentration (1/m³)		Hall mobility (m²/V S)	
Contact type	Continuous	Corner	Continuous	Corner	Continuous	Corner
Annealed in Ar	7.65	10.49	$0.76 \times 10^{22}$	$0.23 \times 10^{22}$	0.011	0.0255
Annealed in H <sub>2</sub>	9.52	13	$0.56 \times 10^{22}$	$0.16 \times 10^{22}$	0.0121	0.029

results in a doped p-type regime. Also, the literature shows that one way of enhancing Al metal contact on Si substrate is to increase the doping level of Si. 26-28 The literature also confirms that below the eutectic temperature of Si and Al (570 °C), Al can form ohmic contacts with p-type Si, because of the small amount of solid-state diffusion of Al into the Si. 30,31

In the as-deposited state, Ti should not diffuse into Si because of very low temperatures during sputtering. As indicated earlier, the Ti on Si was used as an adhesion promotor and diffusion barrier. EDX did not show any diffusion as well after annealing within the detectability limits. It is important to note that the formation of TiAl<sub>3</sub> is more likely to occur in the Al–Ti system after annealing at 450 °C. Similarly, a significant Ti–Si reaction should not occur during annealing at a low temperature of 380 °C, while some intermixing may be possible to promote adhesion and ohmic contact formation.

The Ti–Al films deposited on Si (100) were then annealed in Ar atmosphere at 380 °C for 1 h and I-V characteristics were measured in a manner similar to the as-deposited samples. The results are given in Figs. 6 and 7, respectively, for the continuous and corner contacts. All the I-V curves show linear responses and the correlation coefficient approaching very close to 1. These results indicated that the ohmic contacts of Ti–Al on Si can be readily made after a low-temperature annealing in an inert Ar atmosphere.

Similarly, I-V characteristics were measured after annealing the Ti–Al samples deposited on Si (100) wafers in pure hydrogen gas at 380 °C for 1 h. Both the continuous and corner contacts were investigated. The results are shown in Figs. 8 and 9, respectively, for the continuous and corner contacts. The results show purely ohmic contact resistance for all  $\rm H_2$ -annealed samples, which are similar to postannealing treatment in Argon atmosphere as well.

These I-V behaviors indicated that essentially ohmic contact resistance can be readily obtained for Ti–Al contacts on p-Si (100) by annealing preferably in H<sub>2</sub> atmosphere at low temperatures.

# B. Characterization of properties of p-Si (100) using Ti-Al contact through Hall measurement

The Hall measurement was done using the Ti–Al contact metallization as described in Sec. II B. This approach utilized the Van der Pauw configuration (dot pattern) to measure the properties of the p-Si (100) substrate. All measurements were done at room temperature at different applied magnetic fields and on continuous and corner dot patterns. From these measurements, resistivity, carrier concentration, and Hall mobility of the p-Si (100) were obtained. The following equations describe how these properties were

measured automatically using software as a part of the Lake Shore Hall instrument.

To measure resistivity using the Van der Pauw method, four contact points are used as shown in Fig. 10 for Ti–Al corner contact of type I on Si (100). The procedure for measuring resistivity requires two resistance measurements. For instance, the current source is connected between contacts 2 and 1, and the voltage is measured between contacts 3 and 4. The current is reversed to remove thermoelectric voltages and a current reversed resistance is measured. This is denoted as  $R_{21,34}$  [Eq. (1)]. The current source and voltmeter are rotated to source the current between contacts 3 and 2, and the voltage is measured between contacts 4 and 1. The current is reversed to remove thermoelectric voltages to obtain a current reversed resistance  $R_{32,41}$  [Eq. (2)],

$$R_{21,34} = \frac{V_{34}(I_{21}^+) - V_{34}(I_{21}^-)}{I_{21}^+ - I_{21}^-},\tag{1}$$

$$R_{32,41} = \frac{V_{41}(I_{32}^+) - V_{41}(I_{32}^-)}{I_{32}^+ - I_{32}^-}.$$
 (2)

These two resistance readings are converted to a resistivity by solving the nonlinear equation for the factor "f" to calculate the resistivity [Eqs. (3) and (4)]. Thus, the measured resistivity is the sheet resistivity,

$$\rho_{sheet}^{A} = \frac{\pi f}{\ln(2)} \frac{(R_{21,34} + R_{32,41})}{2}.$$
 (3)

Here, f is the solution to the equation

$$\frac{q-1}{q+1} = \frac{f \cosh^{-1}\left(\frac{e^{\frac{\ln 2}{f}}}{2}\right)}{\operatorname{In}(2)},\tag{4}$$

where

$$q = \frac{R_{21,34}}{R_{32,41}}$$
 or  $q = \frac{R_{32,41}}{R_{21,34}}$ , whichever is larger.

Similarly, resistance  $R_{43,12}$ ,  $R_{43,12}$ , and resistivity [Eqs. (5)–(10)] are obtained by considering other current and



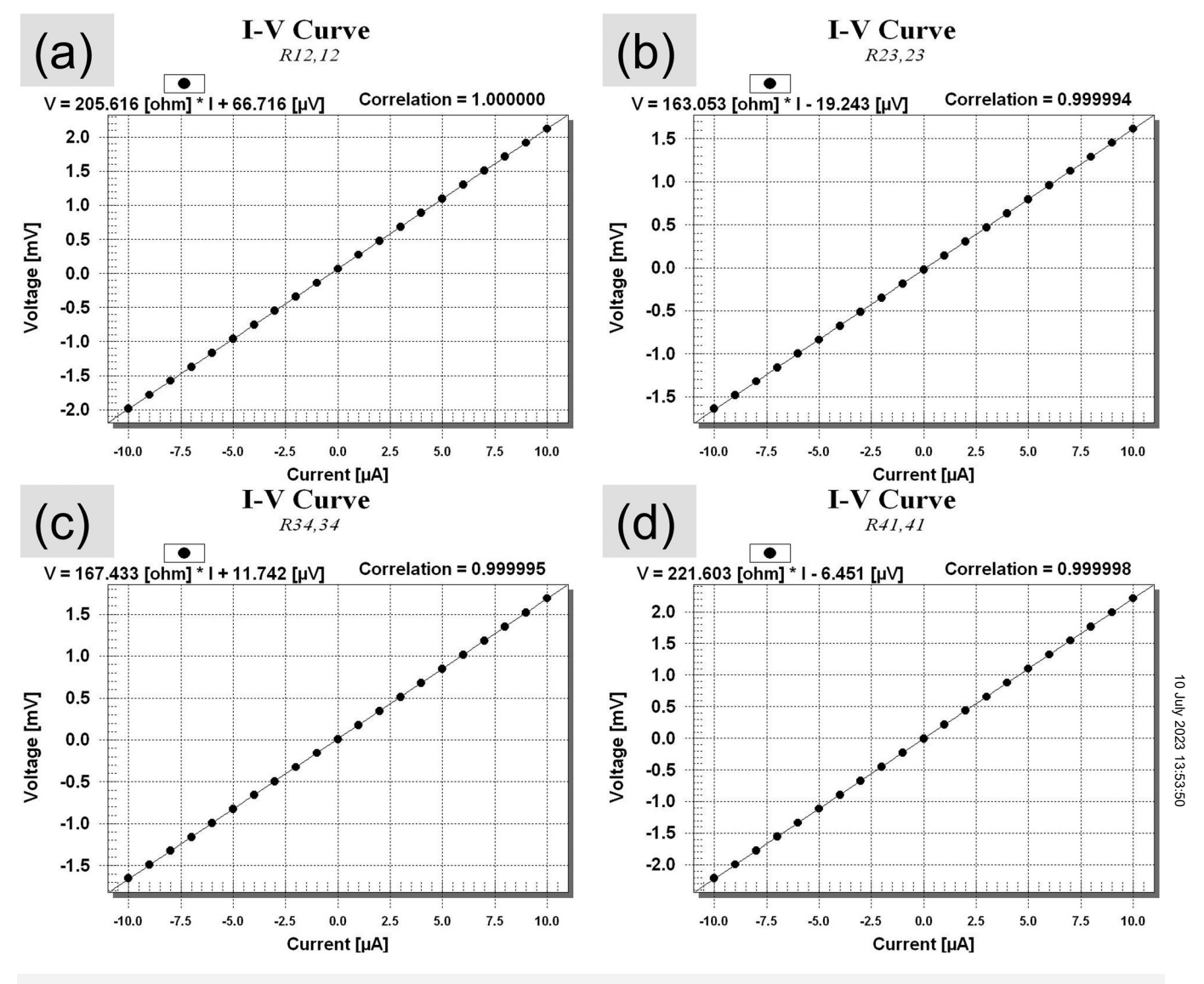


FIG. 6. I-V characteristics of Ti-Al continuous contact of type I on Si (100) after annealing in Ar at 380 °C for 1 h between contacts (a) 1-2, (b) 2-3, (c) 3-4, and (d) 4-1.

voltage contacts as shown in Fig. 11,

Here, 
$$f$$
 is the solution to the equation

$$R_{43,12} = \frac{V_{12}(I_{43}^{+}) - V_{12}(I_{43}^{-})}{I_{43}^{+*}I_{43}^{-}},$$

$$\frac{q-1}{q+1} = \frac{f \cosh^{-1}\left(\frac{e^{\frac{\ln 2}{f}}}{2}\right)}{\ln(2)},$$

$$R_{14,23} = \frac{V_{23}(I_{14}^{+}) - V_{23}(I_{14}^{-})}{I_{14}^{+*}I_{14}^{-}},$$

$$(6)$$

$$\frac{q+1}{q+1} = \frac{f \cosh^{-1}\left(\frac{e^{\frac{\ln 2}{f}}}{2}\right)}{\ln(2)},$$

$$\rho_{sheet}^{A} = \frac{\pi f}{\ln(2)} \frac{(R_{21,34} + R_{32,41})}{2}. \tag{7}$$
 
$$q = \frac{R_{43,12}}{R_{14,23}} \quad or \quad q = \frac{R_{14,23}}{R_{43,12}}, \text{ whichever is larger.}$$

where

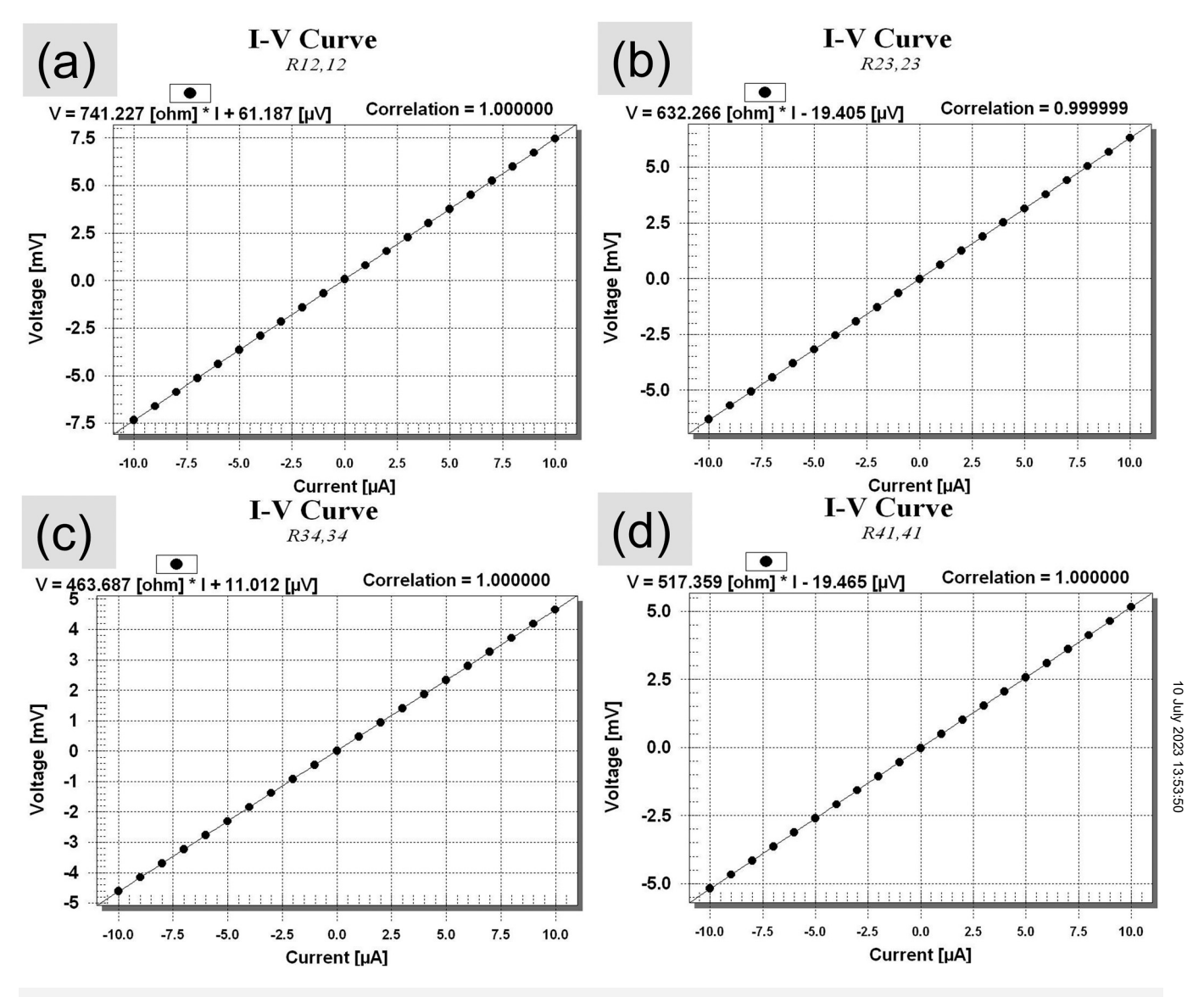


FIG. 7. I-V characteristics of Ti-Al corner contact of type I on Si (100) after annealing in Ar at 380 °C for 1 h between contacts (a) 1-2, (b) 2-3, (c) 3-4, and (d) 4-1.

Thus, the final sheet resistivity is given by

$$\rho = \frac{\rho_{sheet}^A + \rho_{sheet}^B}{2},\tag{9}$$

$$\rho_{bulk} = \rho_{sheet}^* t, \tag{10}$$

*Resistivity* = 
$$\rho_{bulk} = \rho_{sheet}^* t$$
,

where *t* is the thickness of Si.

Further, to measure Hall voltage using the Van der Pauw method, the current source is connected across the diagonal of the sample and the voltage is measured across the other diagonal (see Fig. 12). The voltage is measured at both positive and negative fields as well as positive and negative currents to eliminate misalignment voltages, thereby resulting in four separate measurements. These four measurements are then used to calculate the Hall voltage,  $V_{\rm Hall}$  using Eqs. (11)–(17).

For the current source applied between contact 3 and 1 as shown in Fig. 12(a),

$$V_{13,42}^{B+} = \frac{V_{42}^{B+}(I_{13}^+) - V_{42}^{B+}(I_{13}^-)}{2},\tag{11}$$



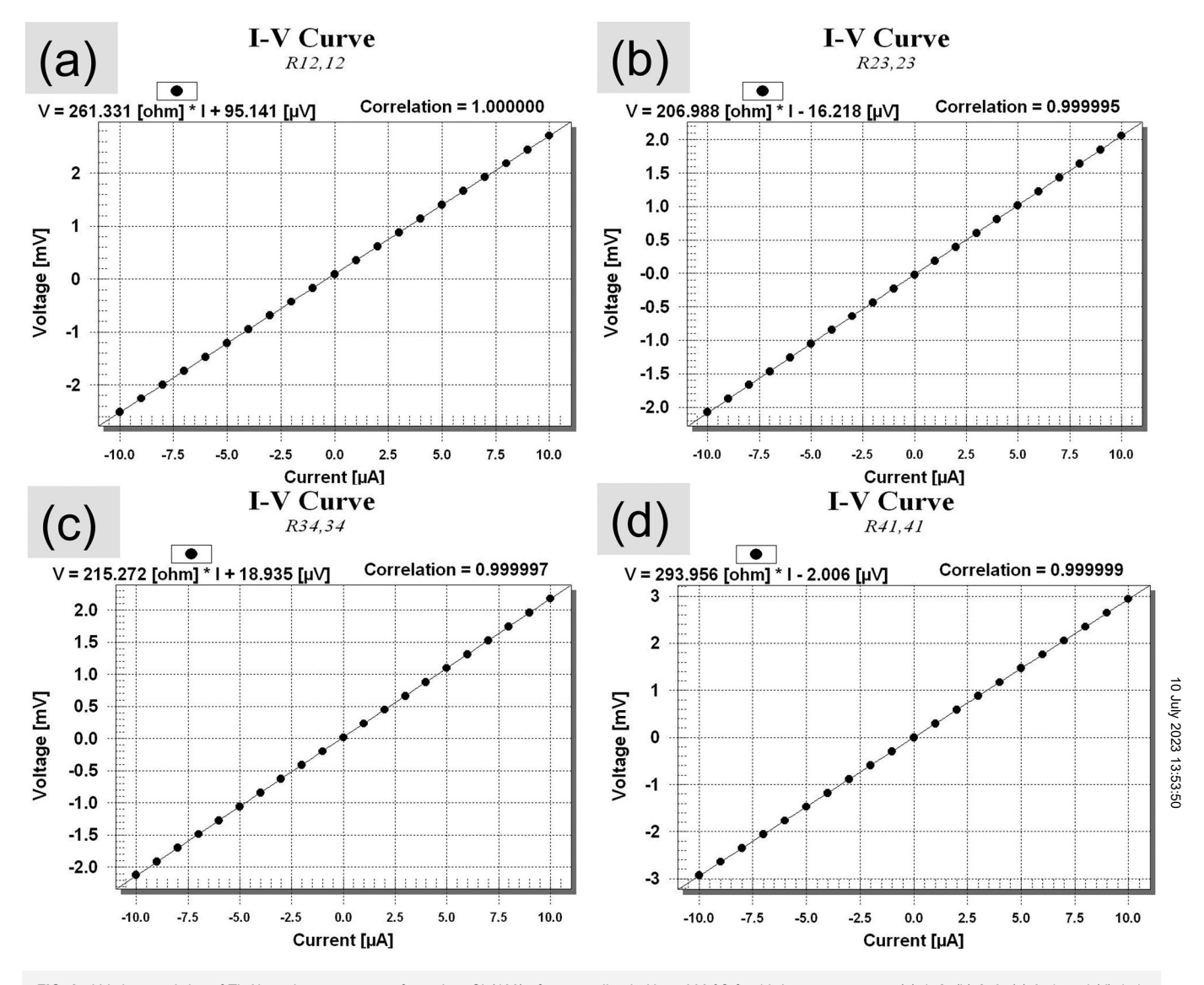


FIG. 8. I-V characteristics of Ti–Al continuous contact of type I on Si (100) after annealing in  $H_2$  at 380 °C for 1 h between contacts (a) 1–2, (b) 2–3, (c) 3–4, and (d) 4–1.

$$V_{13,42}^{B-} = \frac{V_{42}^{B-}(I_{13}^{+}) - V_{42}^{B+}(I_{13}^{-})}{2},$$
(12)

$$V_{AHall} = \frac{V_{13,42}^{B+} - V_{13,42}^{B-}}{2}.$$
 (13)

Similarly, when the current source is applied between contact 2 and contact 4 as shown in Fig. 12(b),

$$V_{24,31}^{B+} = \frac{V_{31}^{B+}(I_{24}^{+}) - V_{31}^{B+}(I_{24}^{-})}{2},$$
(14)

$$V_{24,31}^{B-} = \frac{V_{31}^{B-}(I_{24}^{+}) - V_{31}^{B-}(I_{24}^{-})}{2},$$
(15)

$$V_{BHall} = \frac{V_{24,31}^{B+} - V_{24,31}^{B-}}{2},\tag{16}$$

$$V_{Hall} = \frac{V_{AHall} + V_{BHall}}{2}. (17)$$

 $V_{Hall}$  is related to the fundamental properties as

$$V_{Hall} = \frac{IB_z}{nqt},\tag{18}$$



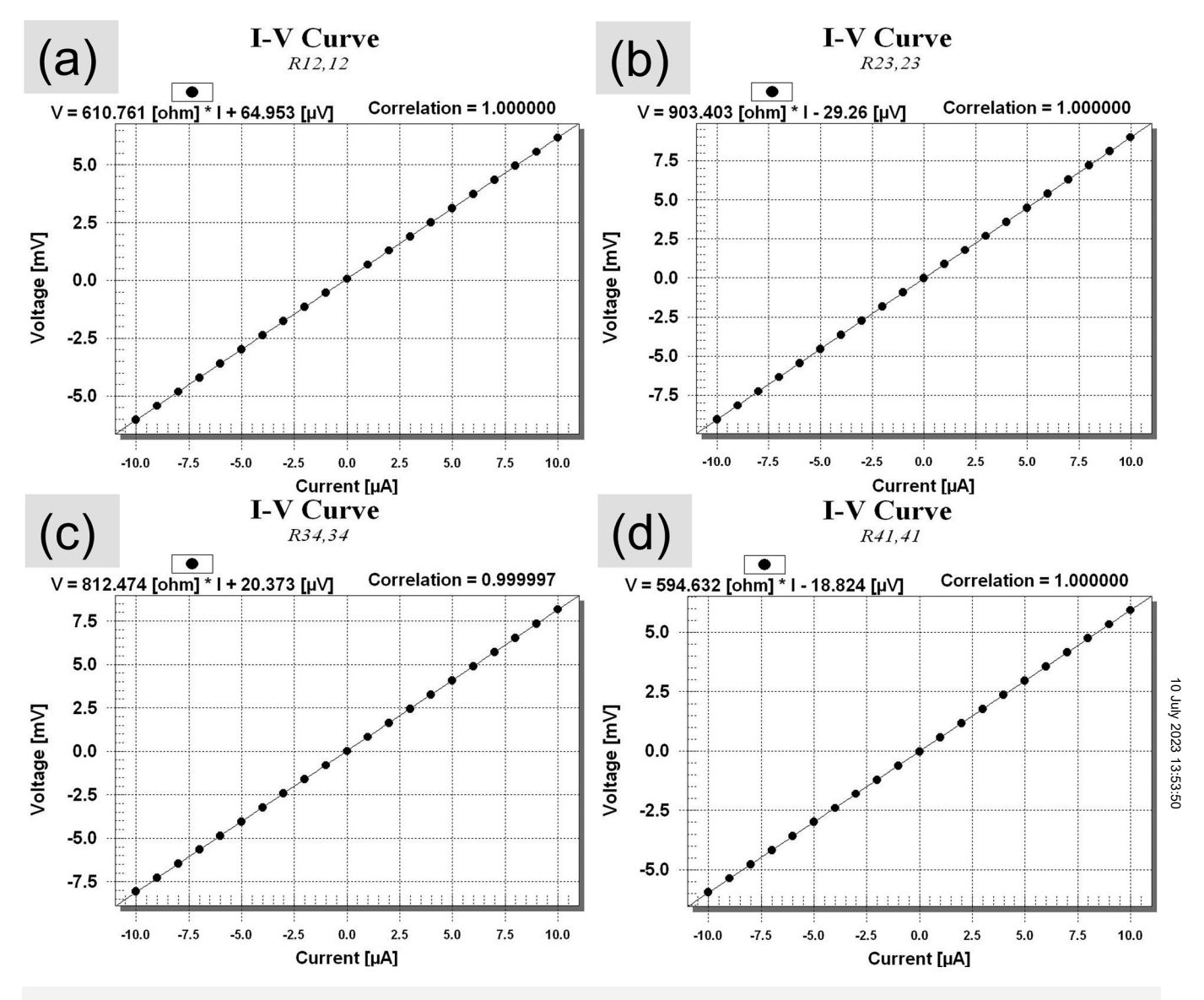


FIG. 9. I-V characteristics of Ti-Al corner contact of type I on Si (100) after annealing in H<sub>2</sub> at 380 °C for 1 h between contacts (a) 1–2, (b) 2–3, (c) 3–4, and (d) 4–1.

where n is the carrier density, t is the thickness of the sample, q is the electronic charge,  $B_Z$  is the magnetic field, and I is the current. The Hall coefficient,  $R_H$ , can be expressed as

$$R_H = \frac{V_{Hall}t}{IB_z}. (19)$$

After we measure the resistivity and Hall coefficient, the carrier concentration and Hall mobility were obtained from the following equations [Eqs. (20) and (21)]:

Carrier concentration = 
$$n = \frac{1}{qR_H}$$
, (20)

Hall mobility = 
$$\mu = \frac{1}{\rho nq} = \frac{R_H}{\rho}$$
, (21)

where n,  $\mu$ ,  $\rho$ ,  $R_H$ , and q represent carrier concentration, Hall mobility, resistivity, Hall coefficient, and carrier charge, respectively.

The electrical properties of the Ti-Al type I contact on Si (100) for the continuous and corner contacts were determined after postannealing in Ar and H2 at 380 °C for 1 h and the results are presented in Fig. 13 and Fig. 14, respectively. The resistivity, carrier concentration, and Hall mobility are found to be independent of the applied magnetic field for all samples tested. Typical values for the Ti-Al type I continuous contact on Si after postannealing in Ar

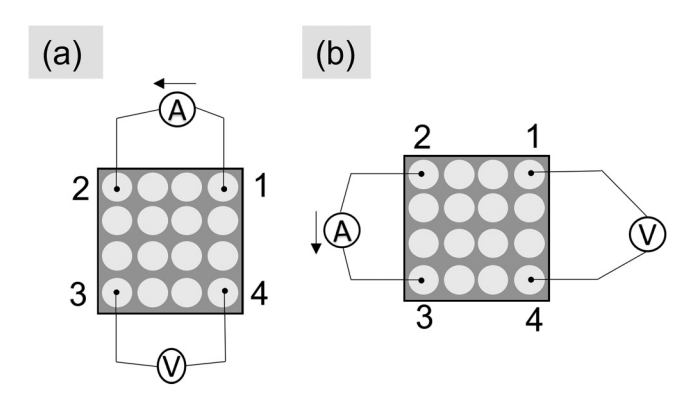


FIG. 10. Sample of Ti-Al with corner contacts of type I on Si (100) showing current (A)-voltage (V) configurations (a) and (b) for resistivity measurements using the Van der Pauw approach.

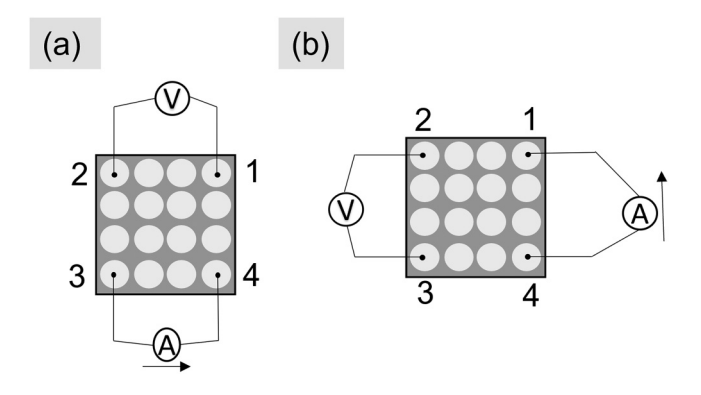


FIG. 11. Current (A)-voltage (V) configurations (a) and (b) for measuring Van der Pauw resistivity of Ti-Al corner contact of type I on Si (100).

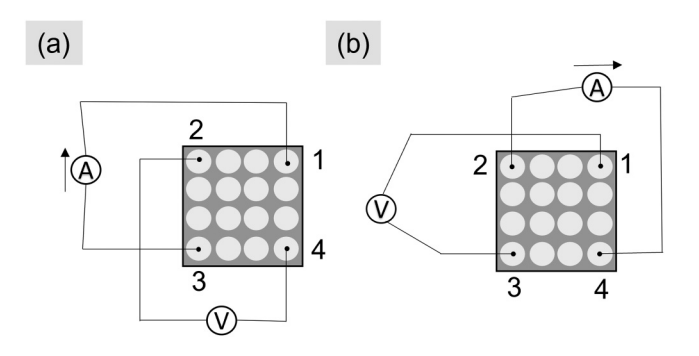
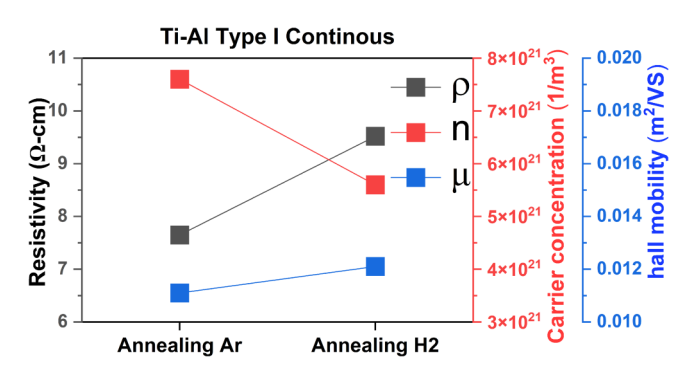


FIG. 12. Current (A)-voltage (V) configurations (a) and (b) for measuring Hall voltage of Ti-Al corner contact of type I on Si (100) using the Van der Pauw method.



**FIG. 13** Resistivity ( $\rho$ ), carrier concentration (n), and Hall mobility ( $\mu$ ) of p-Si (100) in the annealed in Ar and annealed in  $\rm H_2$  at 380 °C for 1 h obtained from the continuous contact dot pattern of Ti-Al metallization through Hall

and  $H_2$  at 380 °C are  $0.56 \times 10^{22}$  m<sup>-3</sup> for the carrier concentration, 0.012 m<sup>2</sup>/VS for the carrier mobility, and 9.52 ohm cm for the resistivity as presented in Fig. 13.

Similarly, for the Ti-Al type I corner contacts after postannealing in Ar and H2 at 380 °C for 1 h, the electrical properties were measured (Fig. 14) as carrier concentration of 0.16 ×10<sup>22</sup> m<sup>-3</sup>, carrier mobility of 0.029 m<sup>2</sup>/VS and resistivity of 13 ohm cm.

A summary of all measured properties of Ti-Al contacts on Si (100) is given in Table II. The I-V data shows that contacts are not ohmic before annealing, so the Hall measurement is not performed on as-deposited samples. After annealing in the atmospheres of Ar 🚊 or H<sub>2</sub>, the contact resistance becomes ohmic. Also, the properties of p-Si (100) wafer extracted after postannealing treatments are similar to those supplied by the vendor of the wafers [diameter— $\frac{3}{20}$ ] 100 mm, thickness— $500 \,\mu$ m, p-type, doping level of boron in  $\frac{1}{20}$  Si (100) is  $0.74 \times 10^{21}$ – $1.67 \times 10^{22}$  m<sup>-3</sup>. Also, mobility and resistivity are in the garden of 0.2260 0.2440  $\frac{1}{200}$ ity are in the range of  $0.0368-0.0418 \text{ m}^2/\text{V S}$  and 1-20 ohm cm]. These results provide a strong justification that the contact metallization should not degrade after the deposition of diamond films on Ti-Al contact metallization useful for power electronic devices based on Si, SiC, and GaN semiconductors. Also, research is

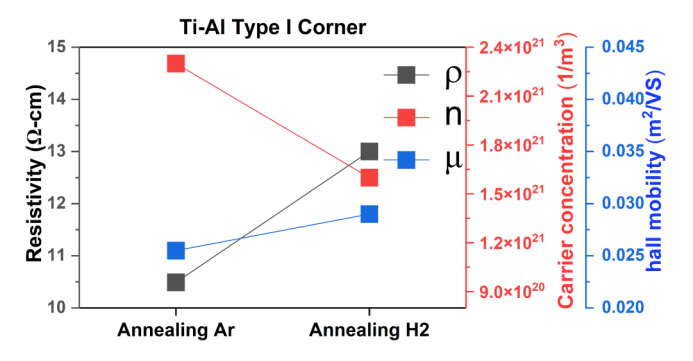


FIG. 14. Resistivity, carrier concentration, and Hall mobility of p-Si (100) in the annealed in Ar and annealed in H2 at 380 °C for 1 h obtained from the corner contact dot pattern of Ti-Al metallization through Hall measurement.

planned on SiC and GaN substrates in support of the suggestion that no degradation should occur to Ti–Al metallization on these wide bandgap semiconductors.

## IV. CONCLUSIONS

Based on the outcomes of Ti–Al contact metallization on p-Si (100) samples, the following conclusions are made.

- 1. Ti–Al films were sequentially deposited on p-Si (100) substrates using the metal mask with circular vias by DC magnetron sputtering using separate pure titanium and aluminum targets. The thickness of Ti was  $\sim$ 10 nm and of Al  $\sim$ 1000 nm.
- 2. The contact resistance and electrical properties of metallized Ti–Al film on silicon were measured before (as-deposited state) and after annealing treatments in argon and hydrogen atmospheres at 380 °C for 1h. The postannealing treatments in argon and hydrogen atmospheres led to pure ohmic contacts and consistent electrical properties, such as lower resistivity, higher carrier concentration, and Hall mobility.
- 3. Typical resistivity values of 7–13 ohm cm, a carrier concentration of  $\sim 1 \times 10^{22}/\text{m}^3$ , and a Hall mobility of  $(1-3) \times 10^{-2} \, \text{m}^2/\text{V}$  S were obtained. These values are close to vendor supplied values for the p-Si (100) wafers.

Future works will focus on the deposition of diamond on metal dot patterns and measure contact resistance and electrical properties of metallized semiconductors after diamond deposition. Current work in progress will include metallized Si, SiC, and GaN substrates that are attractive for the present and future high-power and microelectronic devices.

## **ACKNOWLEDGMENTS**

This research was based on the work supported by the National Science Foundation under NSF Award No. 2122495. Any opinions, findings, and conclusions or recommendations expressed in this material are those of the authors and do not reflect the views of the National Science Foundation.

### **AUTHOR DECLARATIONS**

## **Conflict of Interest**

The authors have no conflicts to disclose.

## **Author Contributions**

Manish Singh: Data curation (equal); Formal analysis (equal); Investigation (equal); Methodology (equal); Validation (equal); Writing – original draft (equal). Lakshmi Narayanan Ramasubramanian: Data curation (equal); Formal analysis (equal); Methodology (equal); Validation (equal). Raj N Singh: Conceptualization (equal); Formal analysis (equal); Funding acquisition (equal); Investigation (equal); Methodology (equal); Project administration (equal); Resources (equal); Supervision (equal); Writing – review & editing (equal).

### **DATA AVAILABILITY**

The data that support the findings of this study are available from the corresponding author upon reasonable request.

### **REFERENCES**

- <sup>1</sup>J. A. Oke and T.-C. Jen, J. Mater. Res. Technol. 21, 2481 (2022).
- <sup>2</sup>O. O. Abegunde, E. T. Akinlabi, O. P. Oladijo, S. Akinlabi, and A. U. Ude, AIMS Mater. Sci. 6, 174 (2019).
- <sup>3</sup>F. M. Mwema, O. P. Oladijo, S. A. Akinlabi, and E. T. Akinlabi, J. Alloys Compd. 747, 306 (2018).
- <sup>4</sup>M. C. Rao and M. S. Shekhawat, Int. J. Modern Phys.: Conf. Ser. 22, 576 (2013).
- §P. Krulevitch, A. P. Lee, P. B. Ramsey, J. C. Trevino, J. Hamilton, and M. A. Northrup, J. Microelectromech. Syst. 5, 270 (1996).
- <sup>6</sup>K. Mech, R. Kowalik, and P. Żabiński, Archiv. Metall. Mater. **56**, 903 (2011).
- <sup>7</sup>M. Muralidhar Singh, G. Vijaya, M. S. Krupashankara, and B. K. S. Sridhara, Mater. Today: Proc. 5, 2696–2704 (2018).
- <sup>8</sup>G. Rincón-Llorente, I. Heras, E. G. Rodríguez, E. Schumann, M. Krause, and R. Escobar-Galindo, Coatings 8, 321 (2018).
- <sup>9</sup>S.-L. Lee, J.-K. Chang, Y.-C. Cheng, K.-Y. Lee, and W.-C. Chen, Thin Solid Films 519, 3578 (2011).
- <sup>10</sup>T. J. Kang, J.-G. Kim, H.-Y. Lee, J.-S. Lee, J.-H. Lee, J.-H. Hahn, and Y. H. Kim, Int. J. Precis. Eng. Manuf. 15, 889 (2014).
- <sup>11</sup>S. Roberts and P. J. Dobson, Thin Solid Films **135**, 137 (1986).
- 12 I. V. Gusev and A. A. Mokhniuk, Vacuum 129, 20 (2016).
- 13E. Abedi Esfahani, H. Salimijazi, M. A. Golozar, J. Mostaghimi, and L. Pershin, J. Therm. Spray Technol. 21, 1195 (2012).
- <sup>14</sup>R.-C. Juang, Y.-C. Yeh, B.-H. Chang, W.-C. Chen, and T.-W. Chung, Thin Solid Films 518(19), 5501–5504 (2010).
- <sup>15</sup>D. Das and R. N. Singh, Int. Mater. Rev. **52**, 29 (2007).
- <sup>16</sup>N. Govindaraju, C. Kane, and R. N. Singh, J. Mater. Res. **26**, 3072 (2011).
- <sup>17</sup>N. Govindaraju and R. N. Singh, Mater. Sci. Eng.: B **176**, 1058 (2011).
- <sup>18</sup>N. Govindaraju and R. N. Singh, in *Processing and Properties of Advanced Ceramics and Composites IV* (American Ceramic Society, 2012), pp. 99–113.
- <sup>19</sup>D. Das, R. N. Singh, S. Chattopadhyay, and K. H. Chen, J. Mater. Res. 21, 2379 (2006).
- <sup>20</sup>N. Govindaraju and R. N. Singh, Comput. Mater. Sci. 43, 423 (2008).
- <sup>21</sup>N. Govindaraju, D. Das, R. N. Singh, and P. B. Kosel, J. Mater. Res. 23, 2774 (2008).
- <sup>22</sup>S. E. Coe and R. S. Sussmann, Diamond Relat. Mater. 9, 1726 (2000).
- <sup>23</sup>Y. Zhou et al., Appl. Phys. Lett. 111, 041901 (2017).
- 24L. J. Van der Pauw, Semiconductor Devices Pioneering Papers (World Scientific, 1991), pp. 174–182.
- **25**L. J. Van der Pauw, Philips Res. Rep. **13**, 1–9 (1958).
- <sup>26</sup>J. Bullock *et al.*, Adv. Energy Mater. **6**, 1600241 (2016).
- 27 H. Ishii, K. Sugiyama, E. Ito, and K. Seki, Adv. Mater. 11, 605 (1999).
- **28**Y. Wan et al., Adv. Energy Mater. 7, 1601863 (2017).
- 29S. A. W. Shah and G. Patrick, presented at the Protocols and Reports, ScholarlyCommons (University of Pennsylvania, 2019).
- <sup>30</sup>M. Siad, A. Keffous, S. Mamma, Y. Belkacem, and H. Menari, Appl. Surf. Sci. 236, 366 (2004).
- <sup>31</sup>H. Rahab, A. Keffous, H. Menari, W. Chergui, N. Boussaa, and M. Siad, Nucl. Instrum. Methods Phys. Res. Sect. A 459, 200 (2001).